Superionic phase transitions and nuclear spin phonon relaxation by Raman processes in $Me_3H(SeO_4)_2$ (Me = Na, K, and Rb) single crystals by ^1H and Me NMR

2007 J. Phys.: Condens. Matter 19 116216

(http://iopscience.iop.org/0953-8984/19/11/116216)

IOP PUBLISHING JOURNAL OF PHYSICS: CONDENSED MATTER

J. Phys.: Condens. Matter **19** (2007) 116216 (13pp) doi:10.1088/0953-8984/19/11/116216

Superionic phase transitions and nuclear spin phonon relaxation by Raman processes in $Me_3H(SeO_4)_2$ (Me = Na, K, and Rb) single crystals by ^1H and Me NMR

Ae Ran Lim

Department of Science Education, Jeonju University, Jeonju 560-759, Korea

E-mail: aeranlim@hanmail.net and arlim@jj.ac.kr

Received 26 November 2006, in final form 2 February 2007
Published 5 March 2007
Online at stacks.iop.org/JPhysCM/19/116216

Abstract

$Me_3H(SeO_4)_2$ (Me = Na, K, and Rb) single crystals were grown by the slow evaporation method, and the relaxation times of the ^1H and Me nuclei in these crystals were investigated using FT NMR spectrometry. The ^1H T_1 NMR results for $K_3H(SeO_4)_2$ and $Rb_3H(SeO_4)_2$ single crystals were very different from those for $Na_3H(SeO_4)_2$ crystals. Short ^1H relaxation times were found for $K_3H(SeO_4)_2$ and $Rb_3H(SeO_4)_2$ at high temperatures, but not for $Na_3H(SeO_4)_2$, which are attributed to the destruction and reconstruction of hydrogen bonds; thus $K_3H(SeO_4)_2$ and $Rb_3H(SeO_4)_2$ have superionic phases, whereas $Na_3H(SeO_4)_2$ does not. The temperature dependence of the relaxation rate for the ^{23}Na nucleus in $Na_3H(SeO_4)_2$ crystals was in accord with a Raman process for nuclear spin–lattice relaxation ($T_1^{-1} \propto T^2$). In contrast, the spin–lattice relaxation rates for the ^{39}K and ^{87}Rb nuclei in $K_3H(SeO_4)_2$ and $Rb_3H(SeO_4)_2$ single crystals exhibited a very strong temperature dependence, $T_1^{-1} \propto T^7$. The motions giving rise to this strong temperature dependence may be related to the high electrical conductivities of these crystals at high temperatures.

1. Introduction

Hydrogen-bonded $Me_3H(SeO_4)_2$ (Me = K, Rb, Cs, and NH_4) crystals are well known for their high protonic conductivities, which increase significantly in their high temperature superionic phases [1]. The conductivities of these crystals are associated with the dynamical disordering of their hydrogen-bond networks, which results in an increase in the number of possible proton positions [2]. Proton conduction occurs in several types of materials, including many hydrogen-bonded systems [3–9]. The most interesting group in the crystal structures of this series is the hydrogen selenate ion, $HSeO_4^-$, which is usually distorted from tetrahedral symmetry

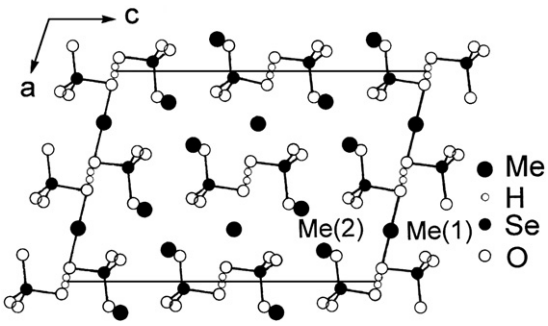

Figure 1. A projection onto the (010) plane of the structure of $Me_3H(SeO_4)_2$ at room temperature.

and takes part in hydrogen bonding. Most crystals in the $Me_3H(SeO_4)_2$ family undergo a superprotonic phase transition from a monoclinic room temperature phase to a trigonal high temperature phase. As the temperature is increased up to the phase transition temperature T_C, the electrical conductivity rapidly increases in the vicinity of the transition temperature, and then decreases according to a power law with further increase of the temperature above the transition temperature. In the paraelastic phase above T_C the conductivity is exceedingly high, as high as that found in ionic conductors [10, 11]. At room temperature, all members of this family are ferroelastic and isomorphous with space group $A2/a$. Above room temperature, they undergo ferroelastic transitions in the range 339–456 K to trigonal ($R\bar{3}m$) paraelastic and superionic phases [12, 13]. Although the physical properties and electrical conductivities of $K_3H(SeO_4)_2$, $Rb_3H(SeO_4)_2$, $Cs_3H(SeO_4)_2$, and $(NH_4)_3H(SeO_4)_2$ crystals have been investigated, the properties of $Na_3H(SeO_4)_2$ crystals have not previously been discussed.

The spin–lattice relaxation time can be used as a measure of the dynamics of a crystal, such as the nucleus–phonon interaction, and indicates how readily the excited state energy of the nuclear system is transferred into the lattice. Thus to obtain information about the structural phase transitions and relaxation processes of $Me_3H(SeO_4)_2$ single crystals, it is useful to measure the spin–lattice relaxation time, T_1, and the spin–spin relaxation time, T_2, in the laboratory frame, and the spin–lattice relaxation time, $T_{1\rho}$, in the rotating frame, for the ^{1}H and Me nuclei. The present study investigated the temperature dependences of T_1, $T_{1\rho}$, and T_2 for the ^{1}H and Me nuclei in $Me_3H(SeO_4)_2$ (Me = Na, K, and Rb) single crystals using pulse NMR spectrometry. The motions of the ^{1}H and Me nuclei at room temperature and in the high temperature phases are discussed in light of these results. The correlation between superionic motion and the relaxation times at high temperatures is also discussed. Further, we consider the correlation between the superionic phase transitions and Raman processes of these $Me_3H(SeO_4)_2$ crystals. The ^{1}H and ^{23}Na NMR properties of the $Na_3H(SeO_4)_2$ crystal are here measured for the first time. We compare these results with those for the $K_3H(SeO_4)_2$ and $Rb_3H(SeO_4)_2$ single crystals, which have similar hydrogen-bonded structures.

2. Crystal structure

$Me_3H(SeO_4)_2$ (Me = Na, K, and Rb) crystals transform from a monoclinic structure with space group $A2/a$ to a trigonal structure with space group $R\bar{3}m$ at high temperatures. The crystal structure of $Me_3H(SeO_4)_2$ at room temperature is shown in figure 1. The structure of $Me_3H(SeO_4)_2$ is built up of hydrogen-bonded SeO_4 dimers and Me cations. There are two

kinds of Me atoms: Me(1) occupies a special position on the twofold axis; Me(2) is at a general position. Both types of Me atoms are surrounded by ten oxygen atoms. A given SeO_4–H–SeO_4 dimer consists of two slightly deformed SeO_4 tetrahedra. The two SeO_4 tetrahedra are connected by a hydrogen bond [14, 15].

3. Experimental method

Single crystals of $Me_3H(SeO_4)_2$ (Me = Na, K, and Rb) were grown with a pseudo-hexagonal plate shape by carrying out the slow evaporation of aqueous solutions containing Me_2SeO_4 and H_2SeO_4. The resulting crystals are hexagonal thin plates, but sometimes exhibit twinning [16, 17]. Transparent plates with dominant (001) faces were obtained. $Na_3H(SeO_4)_2$ crystals are slightly hydroscopic.

The NMR signals of the ^{1}H and Me nuclei in the $Me_3H(SeO_4)_2$ single crystals were measured using the Varian 200 FT NMR and Bruker DSX 400 FT NMR spectrometers respectively, at the Korea Basic Science Institute. The static magnetic fields were 4.7 and 9.4 T respectively, and the central radio frequency was set at $\omega_0/2\pi = 200$ MHz for the ^{1}H nucleus, at $\omega_0/2\pi = 52.94$ and 105.88 MHz for the ^{23}Na nucleus, at $\omega_0/2\pi = 18.67$ MHz for the ^{39}K nucleus, and at $\omega_0/2\pi = 130.93$ MHz for the ^{87}Rb nucleus. For the T_1 measurements, a π–t–$\pi/2$ pulse sequence was used in the ^{1}H, ^{39}K, and ^{87}Rb experiments, whereas a $\pi/2$–t–$\pi/2$ pulse sequence was used in the ^{23}Na experiment. In addition, the $T_{1\rho}$ measurements were obtained using a $\pi/2$–$B_1(t)$ spin-locking sequence with $B_1 = 10$ kHz. The temperature-dependent NMR measurements were obtained over the temperature range 160–450 K. The samples were maintained at a constant temperature by controlling the nitrogen gas flow and the heater current.

4. Experimental results and analysis

From the NMR signals of the ^{1}H ($I = 1/2$) nuclei in the $Me_3H(SeO_4)_2$ crystals, the recovery traces of the magnetizations were measured at several different temperatures. The inversion recovery trace for ^{1}H resonance lines can be represented by the following equation [18]:

$$S(\infty) - S(t) = 2S(\infty)\exp(-t/T_1). \tag{1}$$

The spin–lattice relaxation time, T_1, can be determined directly from the slope of the plot of $\log\{[S(\infty) - S(t)]/2S(\infty)\}$ versus time (t). We found that the inversion recovery traces could be represented by a single exponential form at all temperatures investigated. In addition, the spin–spin relaxation time, T_2, was determined, and the recovery trace of the ^{1}H resonance line can be represented by the expression [18]

$$S(t) = S(\infty)\exp(-t/T_2). \tag{2}$$

We now discuss the recovery laws for quadrupole relaxation in an Me (Me = Na, K, and Rb) nuclear spin system ($I = 3/2$). The transition probabilities for $\Delta m = \pm 1$ and $\Delta m = \pm 2$ are W_1 and W_2 respectively. When the central line is at saturation, the recovery function for the central line is [19–21]

$$S(\infty) - S(t) = S(\infty)[0.5\exp(-2W_1t) + 0.5\exp(-2W_2t)] \tag{3}$$

where $S(t)$ is the nuclear magnetization corresponding to the central transition at time t after saturation. The spin–lattice relaxation rate, $1/T_1$, is given by [22, 23]

$$1/T_1 = [2(W_1 + 4W_2)]/5. \tag{4}$$

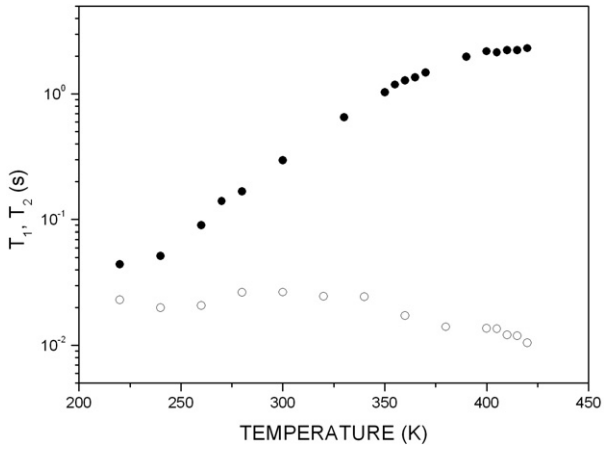

Figure 2. Temperature dependences of the spin–lattice relaxation time, T_1, and spin–spin relaxation time, T_2, for ^{1}H in a $Na_3H(SeO_4)_2$ single crystal (●, T_1; ○, T_2).

4.1. ^1H and ^{23}Na NMR for the $Na_3H(SeO_4)_2$ crystals

To determine the phase transition temperatures of $Na_3H(SeO_4)_2$, differential scanning calorimetry (DSC) was carried out on the crystals using a Dupont 2010 DSC instrument. The measurements were performed at a heating rate of 10 K min^{-1}. No phase transition was found between 120 and 530 K.

The nuclear magnetization recovery curves for ^{1}H were obtained by monitoring the nuclear magnetization after a sequence of pulses at each temperature. From these results, the relaxation time, T_1, in equation (1) was determined directly from the slope of a plot of $\log[(S(\infty) - S(t))/2S(\infty)]$ versus time t. Here, the frequency was set at $\omega_0/2\pi = 200$ MHz. The trace can be nicely fitted with the single exponential function in equation (1). The results for the temperature dependences of the ^{1}H T_1 and T_2 of the single crystal are shown in figure 2. The spin–lattice relaxation time of the ^{1}H nucleus was found to increase with increasing temperature, whereas the spin–spin relaxation time slowly decreases. The spin–spin relaxation time, T_2, of $Na_3H(SeO_4)_2$ crystals is longer than T_2 (on the order of milliseconds) of ^{1}H in the $K_3H(SeO_4)_2$ and $Rb_3H(SeO_4)_2$ crystals. The relaxation times of the ^{1}H nuclei do not undergo significant changes in the investigated temperature range. This result indicates that there are no phase transitions within this temperature range.

The ^{23}Na NMR spectrum consists of a pair of satellite lines and a central line. The resonance lines of ^{23}Na were observed when the magnetic field was applied along the c-axis of the crystal. The two groups in the ^{23}Na spectrum for a frequency of $\omega_0/2\pi = 105.88$ MHz are shown in figure 3. The zero point of the x axis indicates the resonance frequency, 105.88 MHz, of the ^{23}Na nucleus. This result points to the presence of two types of crystallographically inequivalent ^{23}Na nuclei, Na(1) and Na(2). The signal intensities of these groups were found to be similar. The satellite transitions are well resolved from the central line, and the signal intensity of the central line is stronger than those of the other lines. The theoretical intensity ratio of the satellite lines and the central line is 3:4:3, as determined from the transition probabilities [18]. The intensity of the central line observed experimentally is much stronger relative to the intensities of the satellite lines than in the theoretical ratio, due to overlap of the central lines of crystallographically inequivalent Na(1) and Na(2) nuclei. The central transition is virtually unshifted by the quadrupole interaction, and the relationships between the lines

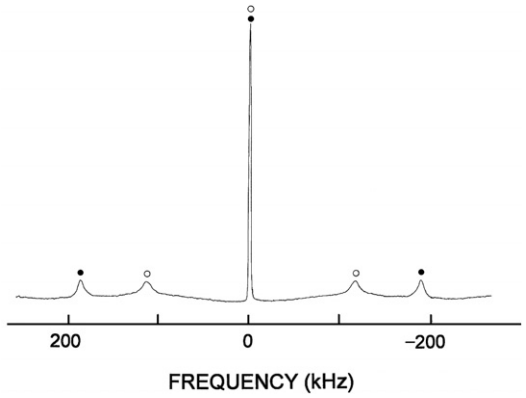

Figure 3. ^{23}Na NMR spectrum at room temperature for $Na_3H(SeO_4)_2$ crystals (●, Na(1); ○, Na(2)).

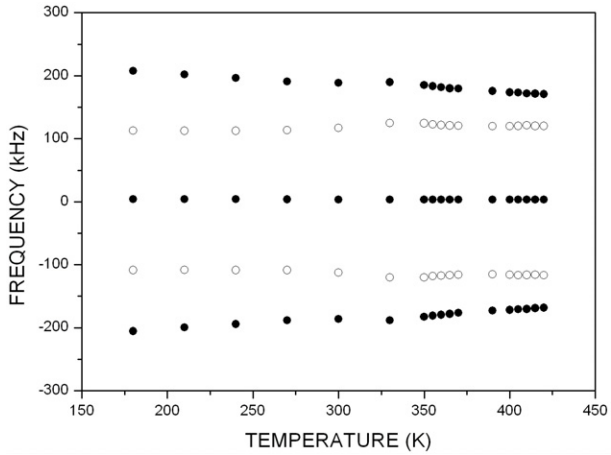

Figure 4. The separation of the ^{23}Na resonance lines as a function of temperature (●, Na(1); ○, Na(2)).

were found to vary with temperature, as shown in figure 4. Usually, the quadrupole coupling constants of ^{23}Na nuclei are on the order of kHz (e.g., the quadrupole parameter of the ^{23}Na nuclei in crystalline $NaMnCl_3$ is 155 kHz [24]). The low quadrupole coupling constants of ^{23}Na nuclei would explain why the central transition is not shifted by the quadrupole interaction. The separation between the resonance lines for one group (○ in figure 4) is nearly constant, whereas the separation between the resonance lines for the other group (● in figure 4) decreases with increasing temperature. Thus the quadrupole parameters of the two crystallographically inequivalent Na(1) and Na(2) nuclei are different. This variation of the separation with temperature is accompanied by distortions of the lattice sites occupied by the Na(1) and Na(2) ions. The variation in the separation of the ^{23}Na resonance lines with temperature indicates that the electric field gradient (EFG) at the Na sites varies with temperature, which in turn means that the atoms neighbouring ^{23}Na are displaced.

The nuclear magnetization recovery curves of the ^{23}Na nucleus were obtained by monitoring the nuclear magnetization after a saturation pulse at several temperatures for a frequency of $\omega_0/2\pi = 52.94$ MHz, and the relaxation time, T_1, in equation (3) was determined

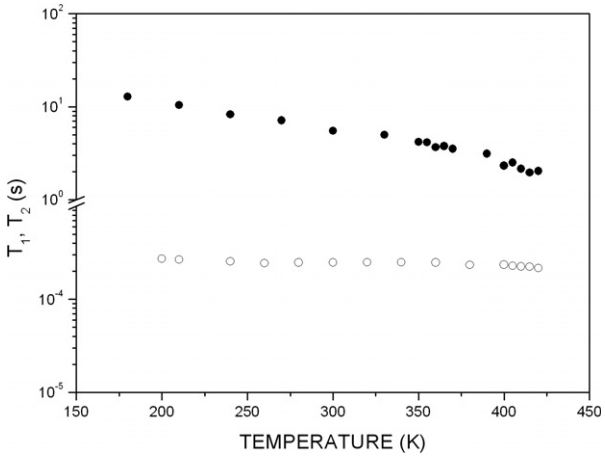

Figure 5. Temperature dependences of the spin–lattice relaxation time, T_1, and spin–spin relaxation time, T_2, for ^{23}Na in a $Na_3H(SeO_4)_2$ single crystal (●, T_1; ○, T_2).

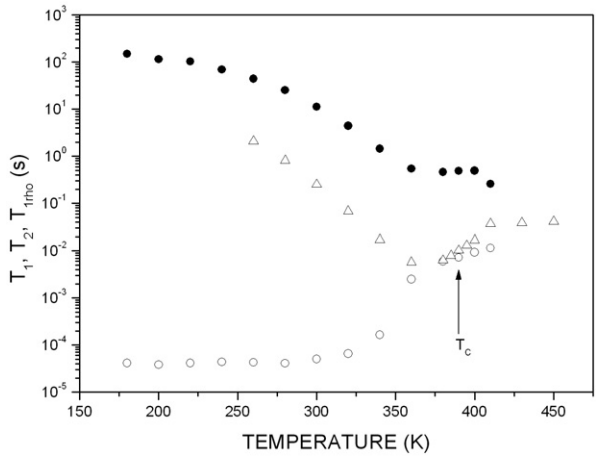

Figure 6. Temperature dependences of the spin–lattice relaxation time, T_1, and spin–spin relaxation time, T_2, in the laboratory frame, and spin–lattice relaxation time, $T_{1\rho}$, in the rotating frame for ^{1}H in a $K_3H(SeO_4)_2$ single crystal (●, T_1; △, $T_{1\rho}$, and ○, T_2).

directly from the slope of the $\log[(S(\infty) - S(t))/S(\infty)]$ versus time t plot. The trace is nicely fitted with the double exponential function in equation (3). The temperature dependences of T_1 and T_2 for the ^{23}Na nuclei are shown in figure 5, and the temperature dependences of the relaxation behaviours of the ^{23}Na nuclei were found to be quite different to those of the ^{1}H nuclei. The T_1 of ^{23}Na slowly decreases with increasing temperature. The spin–spin relaxation time, T_2, is nearly constant with temperature. The spin–lattice relaxation time of ^{1}H was found to be shorter than that of ^{23}Na. Note that T_1 of ^{1}H and ^{23}Na near 400 K have similar values.

4.2. ^{1}H and ^{39}K NMR for the $K_3H(SeO_4)_2$ crystals

The temperature dependences of T_1, $T_{1\rho}$, and T_2 for protons in $K_3H(SeO_4)_2$, obtained by applying a static magnetic field along the crystallographic c-axis, are shown in figure 6. Here

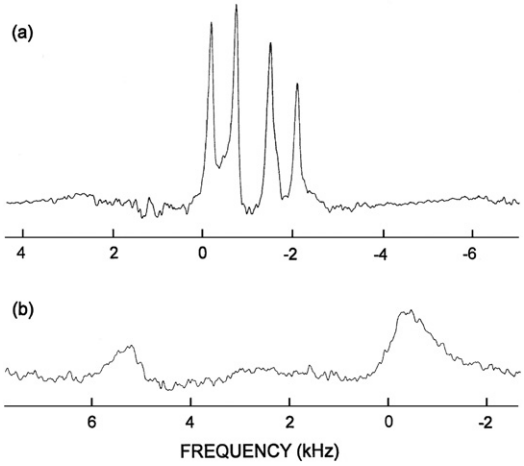

Figure 7. The central lines for crystallographically inequivalent K(1) and K(2) in a $K_3H(SeO_4)_2$ single crystal: (a) four resonance lines indicative of twin domains below T_C and (b) two resonance lines indicative of a single domain above T_C.

the frequency was set at $\omega_0/2\pi = 200$ MHz. The spin–lattice relaxation time, T_1, and the spin–spin relaxation time, T_2, in the laboratory frame exhibit strong temperature dependences. In the ferroelastic phase, T_1 and $T_{1\rho}$ are not governed by the same mechanism. T_1 is governed by the relatively fast $HSeO_4$ rotational reorientations, whereas $T_{1\rho}$ is governed by proton translational motion, which is much slower. The slow translational jumps of protons result in a minimum in the variation of $T_{1\rho}$ with temperature. The minimum in $T_{1\rho}$ was found to occur at 360 K, for $\omega_1\tau_C = 1$ at 5.7 ms, where ω_1 is the spin-locking field strength. At low temperatures, the proton NMR free induction decay is short, indicative of a rigid lattice. As the temperature increases, ω_c (reorientation) speeds up, resulting in a narrowing of the proton NMR linewidth and, as a result, T_2 increases. This increase in T_2 is due to the rapid motion of the protons between the oxygens of each SeO_4 group, giving rise to different, well defined 'orientations' of the $H(SeO_4)_2^{3-}$ ion. Above 390 K, the ^{1}H T_1, $T_{1\rho}$, and T_2 become liquid-like, indicating the presence of translational motion in addition to molecular 'rotation'. The observation of liquid-like values of the proton T_1, $T_{1\rho}$, and T_2 indicates that the phase above T_C is superionic. This is consistent with the appearance of a 'liquid-like' proton T_2 in $(NH_4)_4LiH_3(SeO_4)_4$ and $(NH_4)_4LiH_3(SO_4)_4$, as discussed by Blinc *et al* [25]. These liquid-like T_2 values indicate a drastic motional averaging of the proton dipole–dipole interactions due to translational motion, and are characteristic of superionic states. At temperatures above the phase transition temperature, the crystal lattice changes significantly, as demonstrated by the changes in the proton T_1 and T_2 [26]. The ferroelastic phase is characterized by a correlation time for reorientational motions that is shorter than the correlation time for translational motions. At high temperatures, the reorientational and translational motions are lost, and the proton motion can be characterized with a single correlation frequency ω_c.

The resonance lines of ^{39}K were observed at a frequency of 18.67 MHz. The ^{39}K NMR spectrum has three resonance lines as a result of the quadrupole interactions of the ^{39}K ($I = 3/2$) nucleus. However, four resonance lines were obtained in the temperature range 180–380 K for the ^{39}K nucleus in $K_3H(SeO_4)_2$ crystals instead of three resonance lines, as shown in figure 7(a). The magnitudes of the quadrupole parameters of ^{39}K nuclei are on the order of MHz, so usually only central lines are obtained. Four resonance lines

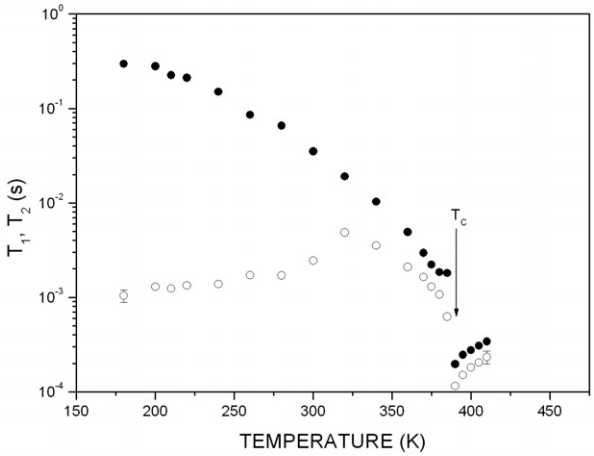

Figure 8. Temperature dependences of the spin–lattice relaxation time, T_1, and spin–spin relaxation time, T_2, of ^{39}K in a $K_3H(SeO_4)_2$ single crystal (●, T_1; ○, T_2).

were obtained for the central transition of the ^{39}K NMR spectrum. This result points to the presence of two types of crystallographically inequivalent ^{39}K nuclei, K(1) and K(2). The other two resonance lines are due to the presence of a ferroelastic domain. Above 390 K, two resonance lines corresponding to the crystallographically inequivalent K(1) and K(2) nuclei are obtained, as shown in figure 7(b). The change to two resonance lines from four resonance lines is associated with the phase transition at 390 K, which indicates that the ferroelastic character has disappeared. The linewidth is broader above T_C than below T_C, and the broad linewidth at high temperatures indicates a shorter T_2 (the linewidth is directly related to the T_2). Further, the separation at high temperatures is larger than at low temperatures, i.e. 6 kHz as compared to 2 kHz. In figure 7(b), one of the lines is close to the position of the lines in figure 7(a) and one line has moved significantly, indicating that the electric field gradient (EFG) for one site changes more than for the other site. From this result, we conclude that the quadrupole parameters of the two types of K nucleus are different. The significant change of the one ^{39}K resonance line at the phase transition temperature of 390 K indicates that the EFG at the ^{39}K sites changes with temperature, which in turn means that the atoms neighbouring the ^{39}K nuclei are displaced from their high temperature positions.

The spin–lattice relaxation time, T_1, and the spin–spin relaxation time, T_2, for the four resonance lines of ^{39}K in $K_3H(SeO_4)_2$ were measured in the ferroelastic and paraelastic phases. The spin–lattice relaxation times were obtained with the saturation recovery method. The recovery traces for the four resonance lines of ^{39}K with dominant quadrupole relaxation can be expressed as a combination of two exponential functions, as in equation (3). The nuclear spin–lattice relaxation time, T_1, for ^{39}K was obtained using equation (4) in terms of W_1 and W_2, and the results are shown in figure 8. The variations with temperature of T_1 for the four resonance lines of K are very similar, and their values are the same within experimental error. The ^{39}K T_1 decrease monotonically with temperature up to 350 K. Further, the spin–spin relaxation time, T_2, was found to depend on temperature. T_2 increases with increasing temperature, and near 320 K starts to decrease with temperature, as shown in figure 8. Above 390 K, the spin–lattice relaxation time and spin–spin relaxation time abruptly decrease, and converge to similar values. This is consistent with the trends in ^{123}Sb T_1 and T_2 of K_2SbF_5, as reported by Panich *et al* [27]. The relaxation times above T_C are in the range expected for a fast-ion conductor with

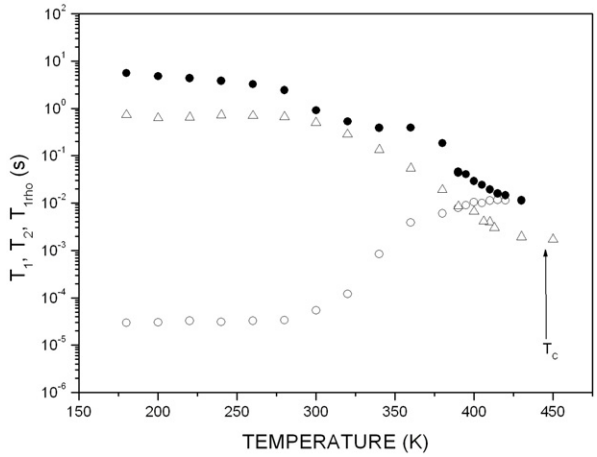

Figure 9. Temperature dependences of the spin–lattice relaxation time, T_1, and spin–spin relaxation time, T_2, in the laboratory frame, and spin–lattice relaxation time, $T_{1\rho}$, in the rotating frame for ^{1}H in a $Rb_3H(SeO_4)_2$ single crystal (●, T_1; △, $T_{1\rho}$, and ○, T_2).

liquid-like particle motion. The spin–lattice relaxation time of ^{1}H was found to be longer than that of ^{39}K. It is expected that the potassium nuclei relax faster than the protons because of their large quadrupolar moments [26].

4.3. ^1H and ^{87}Rb NMR for the $Rb_3H(SeO_4)_2$ crystals

The temperature dependences of the ^{1}H T_1, $T_{1\rho}$, and T_2 in $Rb_3H(SeO_4)_2$ crystals are shown in figure 9, obtained by applying the magnetic field along the c-axis. The spin–lattice relaxation time, T_2, and the spin–spin relaxation time, T_2, have strong temperature dependences. The decrease in $T_{1\rho}$ with temperature can be ascribed to the onset of slow translational motion of the protons. As the temperature increases, ω_c (reorientation) increases, causing a narrowing of the proton NMR linewidth, and T_2 increases. This increase in T_2 is due to protons moving rapidly between the oxygens of one SeO_4 group, giving rise to different, well defined 'orientations' of the $H(SeO_4)_2^{3-}$ ion. In the ferroelastic phase, the ^{1}H NMR measurements of superionic compounds show that $T_2 \ll T_{1\rho} \ll T_1$, with differences of more than an order of magnitude. From the temperature dependences of T_1 and T_2, we conclude that in the ferroelastic phase $\omega_{dip} \ll \omega_c$(reorientation) $< \omega_0$. Here ω_{dip} is the proton Larmor frequency in the local dipolar field (i.e. the dipolar width of the proton line expressed in frequency units), ω_c (reorientation) is the frequency of the rotational motion of the $H(SeO_4)_2^{3-}$ group between different equilibrium orientations, ω_c (translation) is the frequency of the motions of the protons between different sites due to translational motion, and ω_0 is the Larmor frequency in an external magnetic field. At a temperature about 40 K lower than the superionic transition temperature, T_1 is approximately the same as T_2 and $T_{1\rho}$. Therefore, this transition seems to occur at a temperature near 410 K. At high temperatures, there is almost no distinction between the two types of motions; the results show that T_1, $T_{1\rho}$, and T_2 become liquid-like near 400 K, indicating the presence of translational motion in addition to molecular reorientation. The liquid-like values of the ^{1}H T_1, $T_{1\rho}$, and T_2 indicate that the phase above T_C is superionic [28].

Figure 10 shows the ^{87}Rb NMR spectrum of crystalline $Rb_3H(SeO_4)_2$ at room temperature; the magnetic field was applied along the c-axis. Here, the frequency was set at $\omega_0/2\pi =$ 130.93 MHz. When a crystal with crystallographically equivalent nuclei is rotated about the

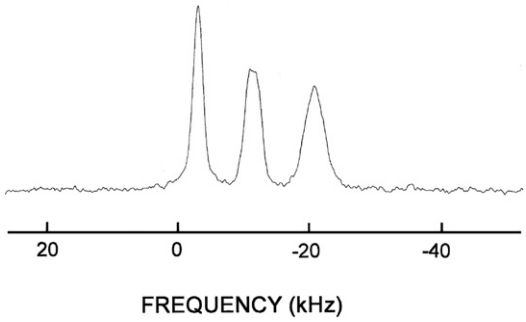

Figure 10. ^{87}Rb NMR spectrum of a $Rb_3H(SeO_4)_2$ single crystal at room temperature.

crystallographic axis, the nuclei give rise to three lines: one central line and two satellite lines. The quadrupole parameters of ^{87}Rb nuclei are usually large enough to be measured in MHz. The two satellite lines for the ^{87}Rb nucleus are located far from the central line, and so are not easy to obtain. Given that $Rb_3H(SeO_4)_2$ contains three types of crystallographically inequivalent ^{87}Rb nuclei, Rb(1), Rb(2), and Rb(2′) [29], the spectrum arising from three types of rubidium nuclei would be expected to contain nine resonance lines. However, only three resonance lines are observed in the temperature range 180–430 K; these resonance lines correspond to the central transition of the ^{87}Rb NMR spectrum for Rb(1), Rb(2), and Rb(2′). One of the three Rb atoms of the formula unit occupies the symmetric Rb(1) site on the twofold axis, whereas the other two atoms Rb(2) and Rb(2′) occupy sites related by a screw axis. The Rb(2) and Rb(2′) sites are chemically equivalent due to the screw axis relation of these two sites, but magnetically inequivalent. This is consistent with the three nonequivalent quadrupole parameters found by Takeda *et al* [30] in the ^{87}Rb NMR spectrum of crystalline $Rb_3H(SO_4)_2$.

The spin–lattice relaxation times of ^{87}Rb in $Rb_3H(SeO_4)_2$ were measured using an inversion recovery sequence; these measurements were conducted only for the central line. The temperature dependences of the spin–lattice relaxation times for the three central lines of ^{87}Rb in $Rb_3H(SeO_4)_2$ were measured. The recovery traces for the three resonance lines of ^{87}Rb with dominant quadrupole relaxation can be represented by a combination of two exponential functions. The nuclear spin–lattice relaxation time, T_1, for ^{87}Rb was obtained using equation (4), and the results are shown in figure 11 as a function of temperature. The T_1 values for the three resonance lines are the same within experimental error. In addition, the spin–spin relaxation time, T_2, was found to depend on temperature. As shown in figure 11, T_2 decreases with increasing temperature, with T_1 and T_2 taking on similar values (i.e. of the order of milliseconds) near 400 K. Unfortunately, in the present study the relaxation time in the laboratory frame could not be determined above 430 K because the NMR spectrometer did not have adequate temperature control at higher temperatures; hence, the phase transition at 446 K could not be detected in the ^{87}Rb T_1 and T_2 NMR results.

5. Discussion and conclusion

$Na_3H(SeO_4)_2$, $K_3H(SeO_4)_2$, and $Rb_3H(SeO_4)_2$ single crystals were grown with the slow evaporation method, and the relaxation times of the ^{1}H, ^{23}Na, ^{39}K, and ^{87}Rb nuclei in these three single crystals were investigated using FT NMR spectrometry. $Na_3H(SeO_4)_2$ crystals do not undergo phase transitions in the investigated temperature range, whereas $K_3H(SeO_4)_2$ and $Rb_3H(SeO_4)_2$ crystals undergo phase transitions at 390 and 448 K respectively. The ^{1}H T_1 NMR results for the $K_3H(SeO_4)_2$ and $Rb_3H(SeO_4)_2$ single crystals are very different from

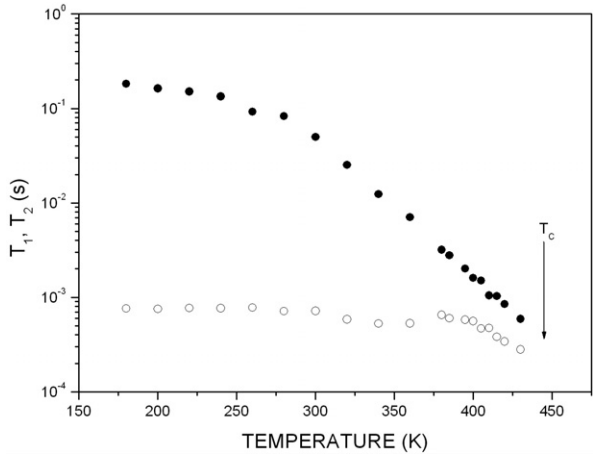

Figure 11. Temperature dependences of the spin–lattice relaxation time, T_1, and spin–spin relaxation time, T_2, of ^{87}Rb in an $Rb_3H(SeO_4)_2$ single crystal (●, T_1; ○, T_2).

those for the T_1 of ^{1}H nuclei in the $Na_3H(SeO_4)_2$ crystals; the T_1 of ^{1}H in $Na_3H(SeO_4)_2$ single crystals increases as the temperature increases, whereas the T_1 for ^{1}H in $K_3H(SeO_4)_2$ and that for $Rb_3H(SeO_4)_2$ single crystals decrease with increasing temperature. Near T_C, T_1, $T_{1\rho}$, and T_2 for ^{1}H in $K_3H(SeO_4)_2$ and $Rb_3H(SeO_4)_2$ are similar, and are indicative of liquid-like systems, with both translational motion and molecular 'rotation' present. At high temperatures the $HSeO_4^-$ reorientations speed up and, because of translational motion, the structure becomes nearly isotropic, the widths of the local polarization distribution and of the correlation time distribution diminish significantly, and the material becomes progressively more plastic. The liquid-like values of T_1, $T_{1\rho}$, and T_2 indicate that above T_C these two crystals are superionic. The short ^{1}H T_1 of $K_3H(SeO_4)_2$ and $Rb_3H(SeO_4)_2$ also indicate that these materials are superionic at high temperatures, because they are indicative of the destruction and reconstruction of hydrogen bonds. Thus, $K_3H(SeO_4)_2$ and $Rb_3H(SeO_4)_2$ have superionic phases, but $Na_3H(SeO_4)_2$ does not. A short spin–lattice relaxation time at high temperatures is usually consistent with the destruction and reconstruction of hydrogen bonds. We suggest that a shift of the hydrogen bound to the oxygen atoms around the selenium atom from its position in the room temperature structure also plays an important role in the phase transition; the phase transition is accompanied by slight rotations of the $H(SeO_4)_2^{3-}$ ions. The proton conduction in $Me_3H(SeO_4)_2$ crystals has been attributed to the hopping of protons, which is accompanied by the destruction and reconstruction of hydrogen bonds. The motion of $HSeO_4$ is associated with the hopping of protons, which makes superionic conduction possible. The structural phase transition at high temperatures may involve the breaking of hydrogen bonds between the nearest SeO_4 tetrahedra and the forming of new weaker disordered hydrogen bonds between neighbouring SeO_4 tetrahedra. This structural phase transition may involve significant reorientation of the SeO_4 tetrahedra and the emergence of dynamical disorder in the hydrogen bonds between them.

The superionic phase transition mechanisms of $K_3H(SeO_4)_2$ and $Rb_3H(SeO_4)_2$ single crystals consist of not only hydrogen hopping, but also of processes involving relaxation via phonons, i.e. those due to librational motions of the selenate tetrahedra. The variation in T_1 with temperature can thus be explained with the relaxation mechanism. Thus the Raman-induced spin–lattice relaxation rate is independent of the Larmor frequency. Using the Debye approximation for the phonon density of states, we obtain [18]

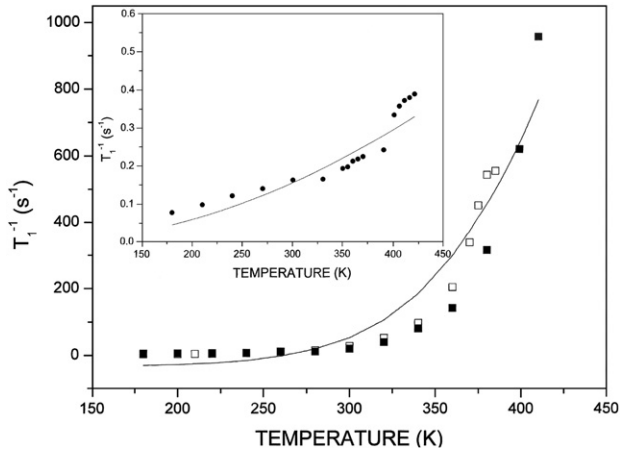

Figure 12. Temperature dependences of the spin–lattice relaxation rates, $1/T_1$, for Me in $Me_3H(SeO_4)_2$ (Me = Na, K, and Rb) crystals (●, Na; □, K, and ■, Rb). The solid lines are fits using the Raman process.

$$\left(\frac{1}{T_1}\right)_{\text{Raman}} = K\int_0^{\theta}\frac{\exp\{T'/T\}}{(\exp\{T'/T\}-1)^2}\left(\frac{T'}{\theta}\right)^6 \mathrm{d}T'. \tag{5}$$

Here θ is the Debye temperature. For temperatures $T \approx \theta$ and higher, equation (5) implies that $T_1^{-1} \propto T^2$, whereas at very low temperatures ($T/\theta \ll 0.02$), the temperature dependence is $T_1^{-1} \propto T^7$. Phonon-induced relaxation is commonly found in electron spin resonance spin–lattice relaxation, but is very rare in nuclear spin relaxation. For the Me nuclei in the three single crystals, the spin–lattice relaxation rate increases as the temperature increases. In the case of $Na_3H(SeO_4)_2$ (see the inset in figure 12), the temperature dependence is of the form of the simple power law $T_1^{-1} \propto T^2$, i.e., it is in accord with a Raman process for nuclear spin–lattice relaxation. However, the spin–lattice relaxation rates for the ^{39}K and ^{87}Rb nuclei of $K_3H(SeO_4)_2$ and $Rb_3H(SeO_4)_2$ single crystals have a very strong temperature dependence, $T_1^{-1} \propto T^7$ (see figure 12). The relaxation process for Me in $Me_3H(SeO_4)_2$ (Me = Na, K, and Rb) crystals is different for different Me. Thus although the $Me_3H(SeO_4)_2$ crystals considered here are all members of the alkali acid selenate family, the $K_3H(SeO_4)_2$ and $Rb_3H(SeO_4)_2$ crystals have superionic phases, but $Na_3H(SeO_4)_2$ does not. Further, the motion giving rise to the strong T_1 temperature dependence, $T_1^{-1} \propto T^7$, of $K_3H(SeO_4)_2$ and $Rb_3H(SeO_4)_2$ may be related to their high conductivities at high temperatures. This suggests that the differences in the chemical properties of Me (=Na, K, and Rb) are responsible for the variations in the natures of the phase transitions and superionic in these crystals. Although $Na_3H(SeO_4)_2$, $K_3H(SeO_4)_2$, and $Rb_3H(SeO_4)_2$ have the same $M_3H(XO_4)_2$ chemical form (M = Na, K, Rb, Cs, and NH_4; X = S, Se), only $Na_3H(XO_4)_2$ crystals possess a very short asymmetrical hydrogen bond [31]. Particular attention has been paid here to $Na_3H(SeO_4)_2$, which is similar to $Na_3H(SO_4)_2$ in possessing a very short hydrogen bond. The length of the hydrogen bond (O–H $\cdots$ O) may be related to the presence and character of the superionic phase at high temperatures.

Acknowledgments

This work was supported by grant no R01-2006-000-10785-0 from the Basic Research Programme of the Korea Science and Engineering Foundation.

References

[1] Haile M, Boysen D A, Chisholm C R and Merle R B 2001 *Nature* **410** 910
[2] Pavlenko N I 1999 *J. Phys.: Condens. Matter* **11** 5099
[3] Kawada A, McGhie A R and Labes M M 1970 *J. Chem. Phys.* **52** 3121
[4] Schmidt V H, Drumeheller J E and Howell F L 1971 *Phys. Rev.* B **4** 4582
[5] Baranov A I, Shuvalov L A and Schagina N M 1982 *JEPT Lett.* **36** 459
[6] Baranov A I, Fedosyuk R M, Schagina N M and Shuvalov L A 1984 *Ferroelectr. Lett.* **2** 25
[7] Blinc R, Dolinsek J, Lahajnar G, Zupancic I, Shuvalov L A and Baranov I A 1984 *Phys. Status Solidi* b **123** k83
[8] Friesel M, Baranowski B and Lunden A 1989 *Solid State Ion.* **35** 85
[9] Baranov A I, Merinov B V, Tregubchenko A V, Khiznichenko V P, Shuvalov L A and Schagina N M 1989 *Solid State Ion.* **36** 279
[10] Matsumoto Y 2001 *J. Phys. Soc. Japan* **70** 1437
[11] Baranov A I, Tregubchenko A V, Shuvalov L A and Schagina N M 1987 *Fiz. Tverd. Tela* **29** 2513
[12] Endo M, Kaneko T, Osaka T and Makita Y 1983 *J. Phys. Soc. Japan* **52** 3829
[13] Ichikawa M, Sata S, Komukae M and Osaka T 1992 *Acta Crystallogr.* C **48** 1569
[14] Melzer R, Sonntag R and Knight K S 1996 *Acta Crystallogr.* C **52** 1061
[15] Gustafsson T, Ichikawa M and Olovsson I 2000 *Solid State Commun.* **115** 473
[16] Yokota S, Makita Y and Takagi Y 1982 *J. Phys. Soc. Japan* **51** 1461
[17] Chen R H, Chang R Y and Shern S C 2002 *J. Phys. Chem. Solids* **63** 2069
[18] Abragam A 1961 *The Principles of Nuclear Magnetism* (Oxford: Oxford University Press)
[19] Igarashi M, Kitagawa H, Takahashi S, Yoshizak R and Abe Y 1992 *Z. Naturf.* a **47** 313
[20] Bonera G, Borsa F and Rigamonti A 1970 *Phys. Rev.* B **21** 2784
[21] Towta S and Hughes D G 1990 *J. Phys.: Condens. Matter* **2** 2021
[22] van der Klink J J, Rytz D, Borsa F and Hochli U T 1983 *Phys. Rev.* B **27** 89
[23] Kim K H, Torgeson D R, Borsa F and Martin S W 1996 *Solid State Ion.* **90** 29
[24] Lim A R, Yeom T H, Choh S H and Jeong S Y 1995 *J. Phys.: Condens. Matter* **7** 7265
[25] Blinc R, Lahajnar G, Seliger J, Zupancic I, Zimmermann M, Fuith A, Schranz W and Warhanek H 1994 *Solid State Commun.* **92** 765
[26] Lim A R and Ichikawa M 2006 *J. Solid State Chem.* **179** 117
[27] Panich A M, Zemnukhova L A and Davidovich R L 2001 *J. Phys.: Condens. Matter* **13** 1609
[28] Lim A R and Ichikawa M 2006 *J. Phys.: Condens. Matter* **18** 2173
[29] Dolinksek J, Mikac U, Javorsek J E, Lahajnar G, Blinc R and Kirpichnikova L F 1998 *Phys. Rev.* B **58** 8445
[30] Takeda S, Kondoh F, Nakamura N and Yamaguchi K 1996 *Physica* B **226** 157
[31] Chen R H, Chen S C and Chen T M 1995 *Phase Transit.* **53** 15